Molecular Biology of the Cell
Vol. 14, 4470–4485, November 2003

Mechanism of Constitutive Export from the Golgi: Bulk Flow via the Formation, Protrusion, and En Bloc Cleavage of large *trans*-Golgi Network Tubular Domains[V]

Elena V. Polishchuk, Alessio Di Pentima, Alberto Luini,* and Roman S. Polishchuk*

Department of Cell Biology and Oncology, Istituto di Ricerche Farmacologiche "Mario Negri," 66030 Santa Maria Imbaro, Chieti, Italy

Submitted January 22, 2003; Revised July 9, 2003; Accepted July 9, 2003
Monitoring Editor: Benjamin Glick

Transport of constitutive cargo proteins from the Golgi complex to the plasma membrane (PM) is known to be mediated by large tubular-saccular carriers moving along microtubules. However, the process by which these large structures emerge from the *trans*-Golgi network (TGN) remains unclear. Here, we address the question of the formation of Golgi-to-PM carriers (GPCs) by using a suitable cluster of morphological techniques, providing an integrated view of their dynamics and three-dimensional structure. Our results indicate that exit from the TGN of a constitutive traffic marker, the VSVG protein, occurs by bulk flow and is a three-step process. First, the formation of a tubular-reticular TGN domain (GPC precursor) that includes PM-directed proteins and excludes other cargo and Golgi-resident proteins. Notably, this step does not require membrane fusion. Second, the docking of this preformed domain on microtubules and its kinesin-mediated extrusion. Finally, the detachment of the extruded domain by membrane fission. The formation of GPCs does not involve cargo concentration and is not associated with the presence of known coat proteins on GPC precursors. In summary, export from the Golgi occurs via the formation, protrusion and en bloc cleavage of specialized TGN tubular-saccular domains.

INTRODUCTION

The *trans*-Golgi network (TGN) is the main sorting station in the secretory pathway for newly synthesized proteins and lipids (Griffiths and Simons, 1986). This is where proteins undergo packaging into membrane carriers for delivery to the cell surface, to the endosomal system, or to secretory granules (reviewed in Keller and Simons, 1997; Mostov *et al*., 2000). Until a few years ago, the formation of all membrane carriers from the TGN was assumed to be driven by vesicular budding (reviewed in Rothman and Wieland, 1996). It is now apparent, however, that post-Golgi carriers serving constitutive transport are complex membranes of variable, but usually large, size, rather than small (60- to 100-nm), round "traditional" transport vesicles (Hirschberg *et al*., 1998; Polishchuk *et al*., 2000). Some look like branching tubules, or tubular clusters, connected to saccular varicosities, whereas others even look like short, flat cisternae 0.5–1.0 μm in length (Polishchuk *et al*., 2000). Further studies (Hirschberg *et al*., 1998; Keller *et al*., 2001; White *et al*., 2001) have shown that Golgi-to-PM carriers (GPCs) segregate out resident Golgi markers, as well as other cargo proteins with different destinations (Keller *et al*., 2001) and that they seem to grow from areas of the TGN devoid of resident proteins that have been called "cargo domains" (Keller *et al*., 2001; White *et al*., 2001).

A crucial question that remains open is how such complex structures form and emerge from the Golgi complex, and in particular, whether their formation involves the budding and homotypic fusion of small vesicles into these larger structures, as has been proposed for endoplasmic reticulum (ER)-to-Golgi transport containers (Bannykh and Balch, 1997).

Here, we attempt to elucidate the mode of formation of GPCs by three main approaches. First, using green fluorescent protein (GFP)-labeled cargo proteins, we observe that GPCs form by cleavage from 1- to 8-μm-long membrane precursors extruded from the Golgi complex along microtubules (MTs) by kinesin. These GPC precursors represent a subdomain of the *trans*-Golgi network (TGN) that at the electron microscopy (EM) level seems to be composed of anastomotic tubular-saccular structures in continuity with the parent Golgi membranes. Second, when membrane (vesicle) fusion is inhibited, bona fide GPC precursors and GPCs continue forming with normal dynamics and structure, and

Article published online ahead of print. Mol. Biol. Cell 10.1091/mbc.E03–01–0033. Article and publication date are available at www.molbiolcell.org/cgi/doi/10.1091/mbc.E03–01–0033.

[V] Online version of this article contains video material for some figures. Online version is available at www.molbiolcell.org.

* Corresponding authors. E-mail addresses: polish@negrisud.it or luini@dcbo.negrisud.it.

Abbreviations used: Ab, antibody; AP, adaptor protein; COP, coat protein; CVEM, correlative video-electron microscopy; EM, electron microscopy; ER, endoplasmic reticulum; GFP, green fluorescence protein; GGAs, Golgi-localizing gamma-adaptin ear homology domain ADP-ribosylation factor-binding proteins; GPC, Golgi-to-PM carrier; MT, microtubule; GalTf, galactosyltransferase; MPR, mannose 6-phosphate receptor; PC-I, procollagen-I; PKD, protein kinase D; PM, plasma membrane; SialTf, sialyltransferase; TG, *trans*-Golgi; TGN, *trans*-Golgi network; VSV, vesicular stomatitis virus; VSVG, G protein of vesicular stomatitis virus.

at normal rates, indicating that they do not arise from the fusion of smaller vesicles. Third, both small (G protein of vesicular stomatitis virus; VSVG) and supramolecular (procollagen-I; PC-I) cargo proteins leave the Golgi within the same GPCs, suggesting that both cargoes use the same mechanism to exit the TGN. Because PC-I aggregates are very large (300–400 nm), this observation agrees with the first two in indicating that the process of GPC formation occurs by direct extrusion of large portions of the TGN. Finally, we find that the formation of GPCs is neither coupled to the concentration of cargo nor is it associated with the recruitment of known adaptor and coat proteins to the GPC precursors budding from the TGN.

These data represent the first integrated description of the dynamics and ultrastructure of the process of formation of post-Golgi carriers destined to the plasma membrane (PM). They indicate that constitutive cargo exits the Golgi by bulk flow through the cleavage of complex tubular-saccular structures from subdomains of the TGN.

MATERIALS AND METHODS

Cell Culture

NRK, Cos7, HeLa, and baby hamster kidney (BHK) cells were cultured in DMEM (Invitrogen SRL, Milan, Italy) supplemented with 10% fetal calf serum and 1 mM L-glutamine. Human fibroblasts (HFs) were cultured in DMEM supplemented with 10% calf serum.

Antibodies and Reagents

Antibodies were obtained from polycolonal antibody (pAb) against the lumenal domain of VSVG from K. Simons (Max Planck Institute, Dresden, Germany); anti-Man II pAb from K. Moremen (University of Georgia, Athens, GA); anti-p97 pAb from G. Warren (Yale University School of Medicine, New Haven, CT); pAb against TGN46 from S. Ponnambalam (University of Dundee, Dundee, United Kingdom); monoclonal antibody (mAb) LF-42 against PC-I (Fisher *et al*., 1995) from L.W. Fisher (National Institutes of Health, Bethesda, MD); mAb against NSF from M. Tagaya (Tokyo University of Pharmacy and Life Science, Tokyo, Japan); mAb against giantin from H.-P. Hauri (University of Basel, Basel, Switzerland); pAbs against GalTf and SialTf from E.G. Berger (Institute of Physiology, University of Zurich, Zurich, Switzerland); pAb against β-COP and the cDNA of galactosyltransferase (GalTf)-cyan fluorescent protein and VSVG-yellow fluorescent protein from J. Lippincott-Schwartz (National Institutes of Health); pAbs against furin and mannose 6-phosphate receptor (MPR) from Affinity Bioreagents (Golden, CO); and mAb against syntaxin-6 from Stressgen Biotechnologies (Victoria, Canada). The mAbs against α-tubulin, γ-adaptin, VSVG, secondary IgG-Cy3 conjugates, and *N*-ethyl-maleimide were from Sigma-Aldrich (Milan, Italy). The cDNA of glutathione *S*-transferase–tagged wild-type and mutant protein kinase D (PKD) were from V. Malhotra (University of California, San Diego, La Jolla, CA). The cDNA of the L294A α-SNAP mutant was from R.D. Burgoyne (University of Liverpool, Liverpool, United Kingdom). The Alexa 488, 546, 633 IgG conjugates, and tetramethylrhodamine B isothiocyanate and fluorescein isothiocyanate dextrans were from Molecular Probes Europe BV (Leiden, The Netherlands). The NANOGOLD gold-antibody conjugates and the GOLDENHANCE-EM kit were from Nanoprobes (Stony Brook, NY).

Cell Transfection and Infection with Vesicular Stomatitis Virus (VSV)

FuGENE 6 reagent (Roche Diagnostics, Indianapolis, IN) or LipofectAMINE 2000 (Invitrogen, Carlsbad, CA) were used for cDNA transfections. The infection of cells with VSV was performed as described previously (Polishchuk *et al*., 2000).

Microinjection

BHK cells transfected with VSVG-GFP or infected with VSV were kept at 40°C for 3 h and then at 20°C for 1.5 h. They were microinjected with 4 mg/ml anti-NSF antibody (clone 2C8) in the presence of fluorescein isothiocyanate or tetramethylrhodamine B isothiocyanate dextrans by using an Eppendorf transjector 5246 (Eppendorf, Milan, Italy) at 20°C, and further incubated at 20°C for 30–40 min to ensure binding of the antibody. Cells were then shifted to 32°C for different times (up to 1 h), to release the VSVG from the Golgi, and they were subsequently labeled with an anti-VSVG mAb.

Fluorescence and Confocal Microscopy

Confocal and time-lapse images were obtained using an LSM510 confocal microscope system (Carl Zeiss, Gottingen, Germany) as described previously (Nichols *et al*., 2001). Live cell images were obtained with a maximal time resolution of 700 ms/frame. Microinjected cells were stained with a Cy3-conjugated anti-VSVG antibody and a polyclonal anti-β-COP antibody (followed by anti-rabbit Cy5) to avoid cross-adsorption with an injected monoclonal anti-NSF antibody. After labeling, cells were optically sectioned into z-stacks. Then, the mean number (± SD) of β-COP-negative carriers containing VSVG was counted in z-sections through the whole thickness of the 20 control and 20 anti-NSF-antibody–injected cells. To estimate VSVG expression on the cell surface, microinjected cells were labeled with a polyclonal anti-VSVG antibody without permeabilization of the cell. Fast videomicroscopy (100 ms/frame) was performed according Keller *et al*. (2001) with an IX70 microscope (Olympus, Hamburg, Germany) equipped with an imaging system (TILL Photonics, Gräfelfing, Germany).

Immuno-EM Analysis, Correlative Video Electron Microscopy (CVEM), and Morphometry

Transfected Cos7 cells were used for immuno-EM identification of TGN exit sites of VSVG-GFP. Briefly, after visualization of VSVG-GFP–positive exit sites by time-lapse confocal microscopy, the cells were fixed, labeled with an antibody against VSVG by using the gold-enhance protocol (Polishchuk and Mironov, 2001), embedded in Epon-812, and cut as described previously (Polishchuk *et al*., 2000). Cryosections were prepared as described previously (Mironov *et al*., 2001). EM images were acquired from thin sections under a Philips Tecnai-12 electron microscope (Philips, Einhoven, The Netherlands) by using an ULTRA VIEW charge-coupled device digital camera. Thin sections of the specimens taken from 20 and 32°C (release of VSVG for 10 min) were used for quantification of gold labeling density of VSVG at the *trans*-Golgi (TG)-TGN and on GPCs.

The *trans*-face of the Golgi stack was identified as that containing clathrin-coated membranes and as being at the Golgi pole opposite the *cis*-element of the Golgi stack, which exhibits a recognizable necklace-like morphology (Rambourg and Clermont, 1990). Moreover, the *cis*-element contained less VSVG (or none) than the rest of the stack at 20°C (see Figure 9A). The density of the gold particles was counted within the *trans*-most cisterna of the Golgi stack and the TGN (20 cells counted in each case). The TGN was defined as ribosomeless membranes adjacent to the *trans*-Golgi cisternae within a distance of 500 nm. Cells used for EM (normal rat kidney [NRK], Cos7, HeLa, BHK, and human fibroblasts) do not exhibit marked differences in their structure of the TGN from each other. Membranes of endosomal origin (usually with transparent lumen and a round shape like multivesicular bodies) were excluded from the counting at the TGN level. In any case, in cell types used in our experiments the endosomal membranes were very scarce in this area (our unpublished data) as indicated by labeling experiments with endocytosed horseradish peroxidase (Griffiths *et al*., 1985).

GPCs are defined as VSVG-containing structures showing no membrane continuity with the Golgi in serial sections and located within 500 nm of the PM. The labeling density was estimated according to Griffiths and Hoppeler, 1986) and expressed as number of gold particles per micrometer of membrane length (mean ± SD).

RESULTS

Characterization of GPC Formation In Vivo by Videomicroscopy

To provide the necessary background to our studies of the mode of GPC formation (see below), the appearance of these carriers was first thoroughly characterized at the light microscopy level in different cell types expressing the G protein of the tsO45 mutant of VSV fused with GFP (VSVG-GFP) (see MATERIALS AND METHODS). The cells were observed under the confocal microscope either 30 min after the 40°C block release, or 10 min after the 20°C block release. GPCs exiting from the Golgi exhibited variable shapes and sizes, showing a continuum from 300-nm-long ovoid objects to 8-μm-long tubules (Figure 1A; Movie 1a), moved toward the periphery in a stop-and-go manner and demonstrated dramatic changes in their shape during this movement. Of note, the introduction of the 20°C block did not change the size, shape, or behavior of the GPCs and is thus not influenced by the ultrastructural changes of the TGN seen at this temperature (Griffiths *et al*., 1985; Ladinsky *et al*., 2002).

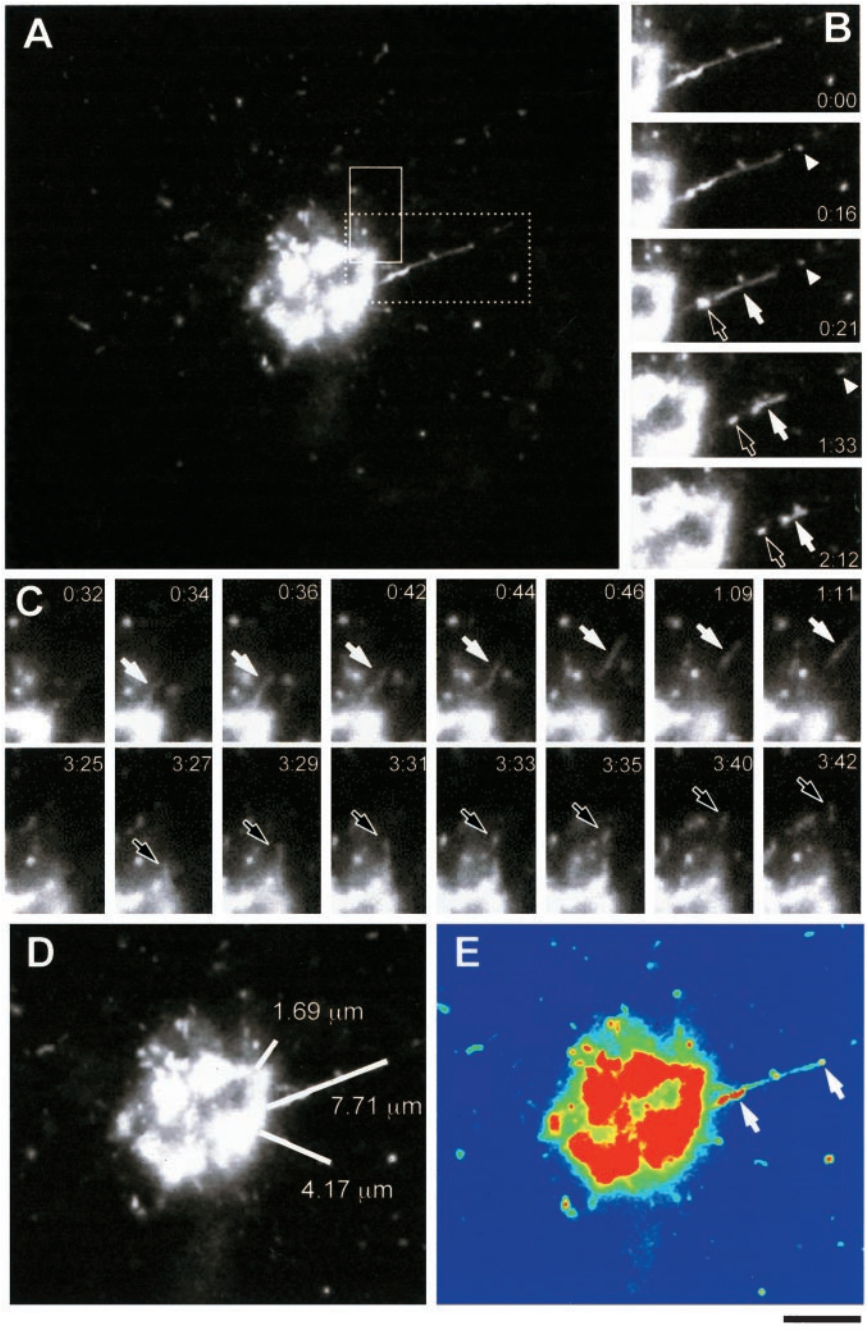

Figure 1. Process of GPC formation. (A) Cos7 cells were transfected with temperature-sensitive VSVG-GFP and kept at 40°C for 4 h and then at 20°C for 2 h, before being shifted to 32°C to initiate transport out of the Golgi. VSVG-GFP exit from the Golgi was observed in specific regions of interest (indicated by boxes) (Movie 1a). (B) Sequential time-lapse images, corresponding to the dashed box region of the cell in A, demonstrate the breakdown of this tubular GPC precursor into three carriers (arrows, arrowhead). (C) Sequential time-lapse images, corresponding to the area defined by the solid box in (A), show the successive formation of two different GPCs (white arrow, black arrow) from the same area of the Golgi. (D) Orientation and length (white lines) of three tubular precursors from which GPCs formed during the course of the observation. (E) The same cell is shown in false colors to indicate the intensity of the VSVG-GFP fluorescence. The arrows indicate the areas of VSVG-GFP concentration within the tubule shown in B. Bar, 4.65 μm (A), 4 μm (B–E).

Many of the VSVG-GFP carriers (~60%) detached from tubule-like structures (Figure 1, A–C; Movie 1a) that extended from the Golgi complex for different distances (from 1 to 8 μm; Figure 1D). Importantly, this extension of VSVG-GFP tubules led to GPC formation in 90% of cases, whereas the remaining 10% of tubules just retracted back toward the Golgi. However, if a VSVG-GFP tubule grew beyond 2.5 μm from the Golgi, it was always transformed into a GPC. We call these tubular structures GPC precursors. Another significant fraction of the GPCs, however, (~40%) seemed to exit from the Golgi mass directly as separate, and sometimes apparently globular, entities. This raised the question whether there might be two different mechanisms of GPC biogenesis (one for the 60% budding from the tubular precursors and the other for this ~40% of GPCs exiting the Golgi abruptly apparently without detaching from tubular precursors). To clarify this issue, the fluorescence within half of the Golgi complex was bleached and the exit of GPCs within this bleached region was monitored. This allowed us to visualize GPC formation events that are usually hidden by extensive fluorescence within the core of the Golgi body. We observed the elongation of many tubules from the nonbleached zone into the bleached region and the subsequent detachment of carriers from such tubular precursors (Figure 2, arrows; Movie 2). Most likely, these are the carriers that seem to exit the Golgi mass as already formed structures. Therefore, this observation suggests that the

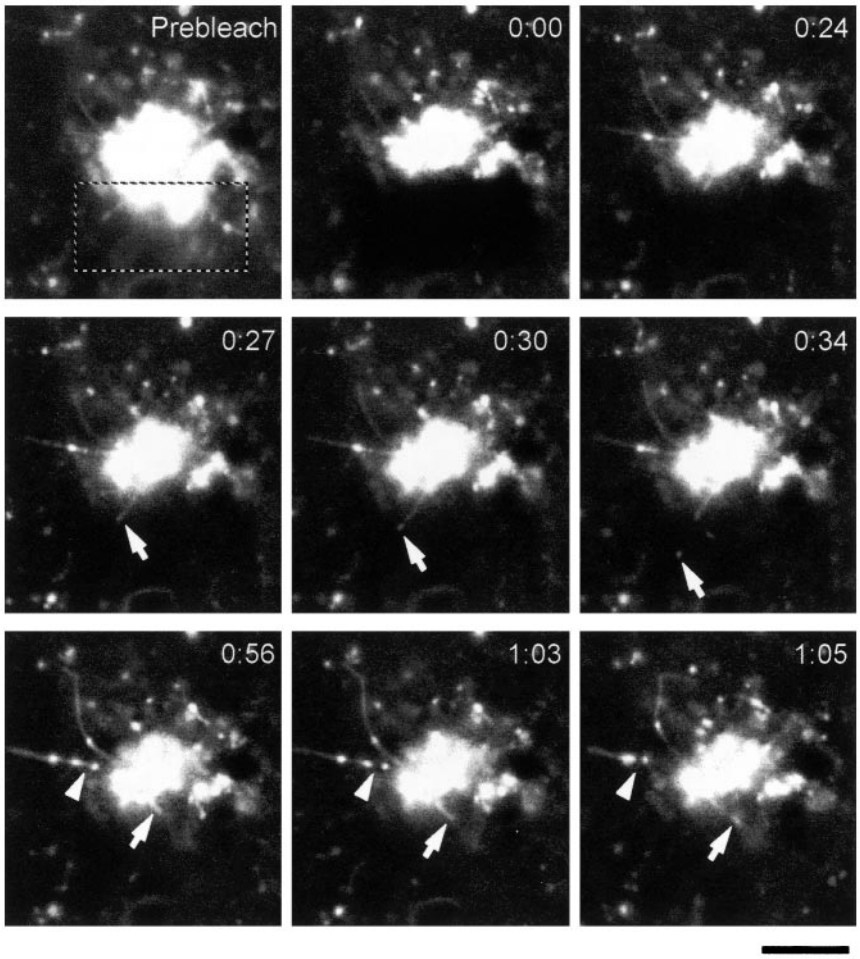

Figure 2. GPC formation within the core region of the Golgi complex. VSVG-GFP transfected Cos7 cells were exposed to the 40°C block for 4 h, shifted to 32°C, and after 30 min observed by confocal microscopy. The portion of the Golgi complex indicated (dashed box) was bleached (Movie 2). Sequential time-lapse images show that formation of GPCs from tubular precursors occurs both in the bleached (arrows) and unbleached (arrowheads) regions. Bar, 4.8 μm.

large majority, if not all, of the VSVG-GFP carriers originate from tubular precursors.

The events of GPC formation had extremely variable durations, ranging from 2 to 200 s after the beginning of tubule extension from the Golgi. When formation events took a longer time, tubular precursors frequently moved in a stop-and-go manner before GPC fission. Notably, detachment of GPCs occurred only when their TGN tubular precursors were being stretched out and away from the Golgi mass. No scission of GPCs from their tubular precursors was ever observed when they were seen not to be moving. Sometimes, we also observed the breakdown of long tubular precursors into two or three GPCs (Figure 1B). The cleavage of these carriers usually happened between fluorescent "hot spots" of VSVG-GFP signal on the tubular precursors (Figure 1E, arrows; Movies 1, a and b). Such hot spots corresponded, at the EM level, to complex areas of convoluted and branching membranes (see below), and were associated with kinesin (see below). Interestingly, the movement of these spots within the same GPC precursor was often nonsynchronous (Movie 1b; arrowheads), i.e., while one was moving (probably pulled by kinesin), the neighboring hot spot would often remain immobile or move at a lower speed. As a result, this segment of a GPC precursor between two hot spots seemed to be stretched. Together, therefore, these observations suggest a link, not previously reported, between the stretching of the GPC precursors and the fission event (see DISCUSSION).

The extension of tubules that subsequently led to the formation of GPCs occurred repetitively from the same points of the Golgi body (arrowheads in Movies 3a and 5). The rate of tubule extension was usually in the range of 0.2–1.5 μm/s, which is similar to that reported for GPC translocation along MTs (Hirschberg *et al*., 1998, Toomre *et al*., 1999). This suggested that MTs play a role in defining the sites of GPC exit from the Golgi and that kinesin might provide a force to pull GPC precursors along MTs. To examine this possibility, living cells were fixed when they exhibited GPC precursors elongating from the TGN, and before detachment of a GPC (Movie 3a). The arrangement of these GPC precursors was compared with the pattern of MTs labeled with tubulin. Figure 3A demonstrates that all such tubular GPC precursors were oriented along MTs. Moreover, the tubular GPC precursors growing from the Golgi were labeled for kinesin both at their tips and at sites corresponding to hot spots (see above) of VSVG-GFP signal (Figure 3, B–D; Movie 3b). Kinesin was also found on free GPCs in the cell cytoplasm, whereas the Golgi complex itself was not labeled (Figure 3D). Thus, the extrusion of tubular GPC precursors occurs along MTs and seems to be driven by kinesin.

To address the question whether GPC precursors might emerge as particular domains of Golgi membranes that are involved in the packaging of secretory material, we examined the composition of GPC precursors by testing for the presence of a number of Golgi markers. As expected, emerg-

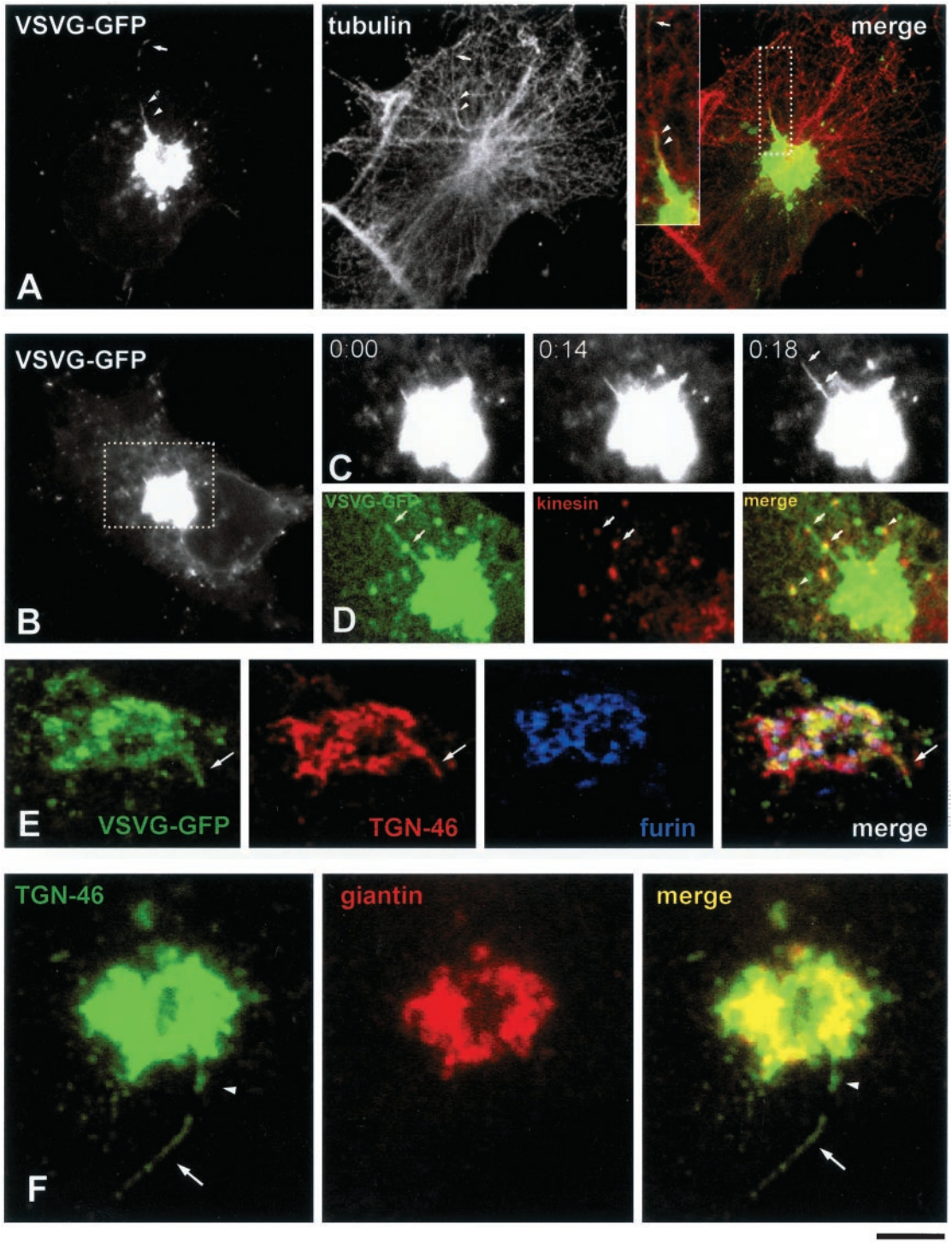

Figure 3. Molecular composition of GPC precursors and their association with microtubules. (A) A VSVG-GFP–transfected Cos7 cell was exposed to the 40 and 20°C blocks, shifted to 32°C, fixed just after the detachment of a GPC from its tubular precursor (Movie 3a), and then stained with an antibody against α-tubulin. Both the GPC (arrow) and the tubular domain of its exit from the Golgi (arrowheads) are oriented along microtubules. Inset, right, detail of the Golgi region corresponding to the dashed box region. (B) Formation of a GPC was observed in the Golgi region (dashed box) of a Cos7 cell transfected with VSVG-GFP (Movie 3b). (C) Time-lapse images, corresponding to the dashed box region of the cell in B, show a tubular GPC precursor (arrows) extending from the Golgi. (D) The same GPC precursor in C was fixed and stained for kinesin. Immunolabeling indicates the presence of kinesin on the hot spots of GPC precursors (arrows) and free GPCs (arrowhead). (E) A Cos7 cell transfected with VSVG-GFP was observed under confocal microscopy until a GPC precursor (arrow) started to bud from the Golgi (Movie 3d). At this moment, the cell was fixed and stained for TGN46 and furin. Distribution of these markers revealed that the GPC precursor contains TGN46, but does not contain furin (arrow). (F) A Cos7 cell grown under steady-state conditions (no temperature blocks, no VSVG-GFP transfection) was fixed and stained for TGN46 and giantin. A free tubule (arrow) and a tubule attached to the Golgi (arrowhead) are seen to contain TGN46 and to exclude giantin. Bar, 7 μm (A and B), 4.3 μm (C and D), 4 μm (E), and 2.9 μm (F).

ing VSVG-GFP tubules were not labeled for Golgi resident proteins, such as mannosidase II, GalTf, and sialyltransferase (SialTf) (Movie 3c), nor for a number of TGN marker proteins such as furin, MPR, and syntaxin 6. Also, all the known coat proteins were absent (see below). The only exception was TGN46, which was found in all VSVG-GFP–positive GPC precursors budding from the Golgi (Figure 3E, arrow; Movie 3d). Thus, TGN46, an endogenous protein that is known to cycle between the TGN and the PM (Banting and Ponnambalam, 1997), apparently uses the same TGN exit sites as VSVG-GFP. Therefore, GPCs form from domains of the TGN membranes which contain TGN46 and partition out many other TGN molecules.

Importantly, these features of the GPC precursors were independent of the experimental protocol used and on the degree of expression of VSVG (our unpublished data). Moreover, in cells not expressing VSVG, tubular TGN46-containing structures reminiscent of GPC precursors (Figure 3F, arrowhead) and GPCs (Figure 3F, arrow) were also seen. This suggests that the shape and dynamics of GPC precursors do not depend on the abundance, or even the presence, of VSVG.

GPC Formation Does Not Require Fusion of Small Vesicles

Based on the above-mentioned observations, at least two main schemes can be proposed to explain the formation of GPCs. First, GPC precursors could form by direct protrusion of complex convoluted tubular structures at the TGN, which then bind to kinesin, and unfold and move out along MTs. Alternatively, they could form by budding and homotypic fusion of small vesicles at the TGN, similar to the scheme proposed for pre-Golgi carriers forming at ER exit sites (Bannykh and Balch, 1997), and then translocate away along MTs. To distinguish between these two possibilities, we tested whether assembly of GPCs requires fusion of vesicles at the TGN. This was achieved by blocking membrane fusion by using specific reagents. We first microinjected BHK cells with a neutralizing antibody against NSF (an ATPase essential for numerous fusion events). Because this antibody has been shown to act potently and specifically in hamster cells (Fukunaga *et al*., 1998), the BHK cell line was used for these experiments. The antibody was effective in blocking brefeldin A-induced fusion of Golgi and ER membranes (our unpublished data). Next, the antibody was microinjected into VSV-infected BHK cells during the course of the 20°C block; the cells were then shifted to the permissive temperature for 30 min. Cell-surface staining with an antibody against the ecto domain of VSVG showed that VSVG delivery from the Golgi to the PM, and hence GPC fusion with the PM, was strongly inhibited in antibody-injected cells, confirming the effectiveness of this reagent (Figure 4, A and B, arrows; and C). Finally, the effect on GPC formation of the anti-NSF antibody was examined under the same conditions. The formation of GPCs was not inhibited. Indeed, microinjected cells exhibited an accumulation of VSVG carriers within the cytoplasm (Figure 4, D and E), most likely due to the fact that carriers could form but not fuse with the PM. These accumulated carriers did not result from nonspecific fragmentation of the Golgi or from a block of ER-to-Golgi transport because the majority of them did not label for β-COP (Figure 4E), SialTf, or γ-adaptin. Similar results were obtained by blocking the NSF cofactor α-SNAP; microinjection of the α-SNAP L294A mutant did not perturb exit of VSVG carriers from the Golgi, but did inhibit their fusion with the PM (our unpublished data). Another ATPase, p97, has been reported to be involved in early Golgi fusion events (Acharya *et al*., 1995; Rabouille *et al*., 1998) and cannot formally be excluded as playing a role in GPC biogenesis. However, microinjection of a neutralizing anti-p97 antibody (Rabouille *et al*., 1998) affected neither GPC formation nor their fusion with the PM (our unpublished data). This is consistent with data from another laboratory that shows that transfection of an ATP-locked mutant of p97 does not affect VSVG-GFP delivery to the PM (Hanson, personal communication).

We also examined directly in living cells whether the dynamics of GPC formation was affected by the anti-NSF antibody. In these cells, GPCs emanated from the VSVG-GFP–positive tubular precursors with similar morphology (Figure 5, A and B; Movie 5) and kinetics (Figure 5C) to control cells. GPCs kept forming for up to 60 min, consistent with the occurrence of several GPC formation cycles.

Finally, we examined the ultrastructure of the GPCs formed in the anti-NSF-antibody–microinjected cells. This is necessary because these GPCs might in fact consist of compact clusters or rows of vesicles unable to fuse with each other, a possibility that cannot formally be excluded by fluorescence microscopy because of the insufficient resolution power of this technique. To this end, microinjected cells expressing VSVG-GFP were prepared for immuno-EM. This showed that both in control and microinjected cells GPCs have similar sizes (Figure 5D) and the same complex tubular-saccular morphology (Figure 5, E and F, arrows) and that they exhibit clearly visible fenestrae (Figure 5, E and F, arrowheads), as would be expected of membranes deriving from a protrusion of the TGN. No accumulation of scattered or clustered VSVG vesicles was observed in microinjected cells. Therefore, the blockade of fusion does not affect the formation of VSVG containers from the Golgi, indicating that this process does not involve budding and fusion of vesicles at the TGN level.

PC-I Aggregates and VSVG Exit the Golgi within the Same GPCs

Another approach toward clarification of the mechanism of GPC formation was to examine whether PC-I aggregates can exit the Golgi complex in the VSVG-carrying GPCs. If so, this would support the conclusion that GPCs derive from direct extrusion of large TGN domains without a need for vesicle fusion (300-nm-long PC-I aggregates do not fit into regular 50- to 100-nm vesicles).

To test this possibility, the human fibroblast (HF) cellular system was used, which allows the synchronization of the transport of PC-I and VSVG (Mironov *et al*., 2001). HFs were infected with VSV and exposed to the 40 and 20°C blocks. At the end of the 20°C block, both PC-I and VSVG were efficiently accumulated within the Golgi complex (Figure 6A). This was confirmed at the EM level, where Golgi stacks were labeled with an anti-VSVG antibody and exhibited 300- to 400-nm-long extensions, indicating the presence of PC-I aggregates (Figure 6C, arrow).

The release of the 20°C block resulted in the exit of GPCs from the Golgi (Figure 6B). Immunostaining revealed strong colocalization of PC-I and VSVG within the same GPCs (Figure 6B). This observation suggests that VSVG leaves the TGN within the large membrane structures that also contain the PC-I aggregates, which cannot themselves be physically incorporated into small, 50- to 100-nm vesicles. Many of the GPCs contained globular parts that were labeled for both PC-I and VSVG, and tubular parts that were only VSVG positive (Figure 6B, arrows). By EM, GPCs forming at the

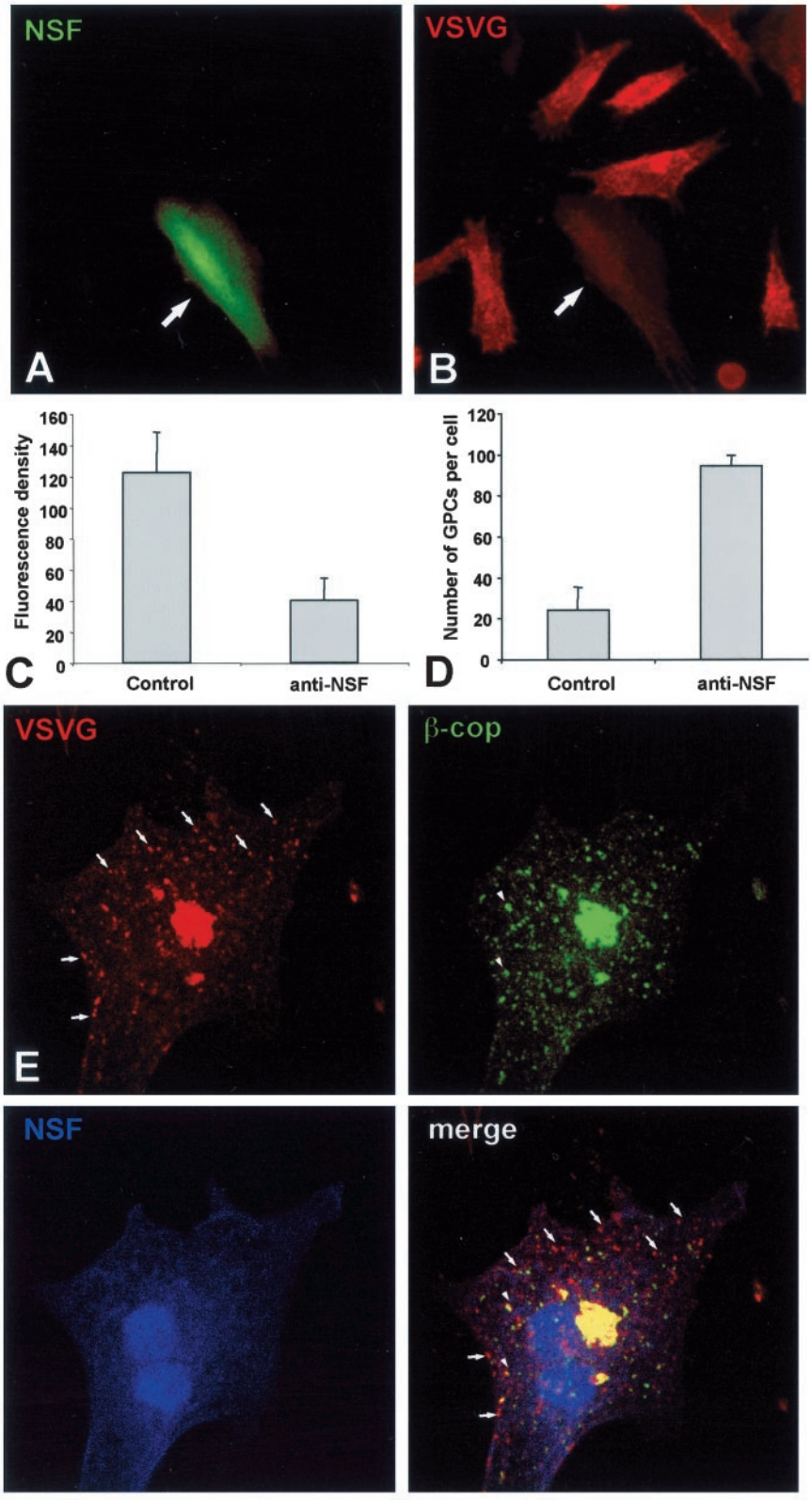

Figure 4. Post-Golgi transport of VSVG after microinjection of an anti-NSF antibody. (A and B) BHK cells were infected with VSV, exposed to the 40°C block, and microinjected with an anti-NSF antibody (mixed with fluorescent dextran) during the 20°C block. They were then shifted to 32°C for 30 min, fixed, and stained with an antibody against the ectodomain of VSVG without permeabilization. The microinjected BHK cell (arrows) exhibits less VSVG signal on its cell surface in comparison with the noninjected cells in B. (C) Fluorescence density of VSVG surface staining (mean ± SD) was quantified in mock-injected (n = 35) and anti-NSF-antibody–injected (n = 35) cells (arbitrary units), treated as in A and B. (D) Cells were infected with VSV, treated as in A and B, fixed, permeabilized, and stained with an anti-VSVG antibody conjugated with Cy3. The number of GPCs (mean ± SD) in mock-injected (n = 20) and anti-NSF-antibody–injected (n = 20) cells 30 min after the release of the 20°C block are shown. (E) A BHK cell was infected with VSV, microinjected at 20°C, shifted to 32°C for 30 min, and then fixed, permeabilized, and stained for VSVG and β-COP. Numerous β-COP–negative GPCs have accumulated within the cytoplasm of the injected cell (arrows). Bar, 34 μm (A and B) and 12 μm (E).

TGN (Figure 6D) exhibited large PC-I distensions (arrowhead) connected to the VSVG-labeled tubules (arrow). These data suggest that PC-I–containing GPCs exit the Golgi as a result of the detachment of TGN membranes that possess significant tubular components interconnected with saccular areas where PC-I can reside.

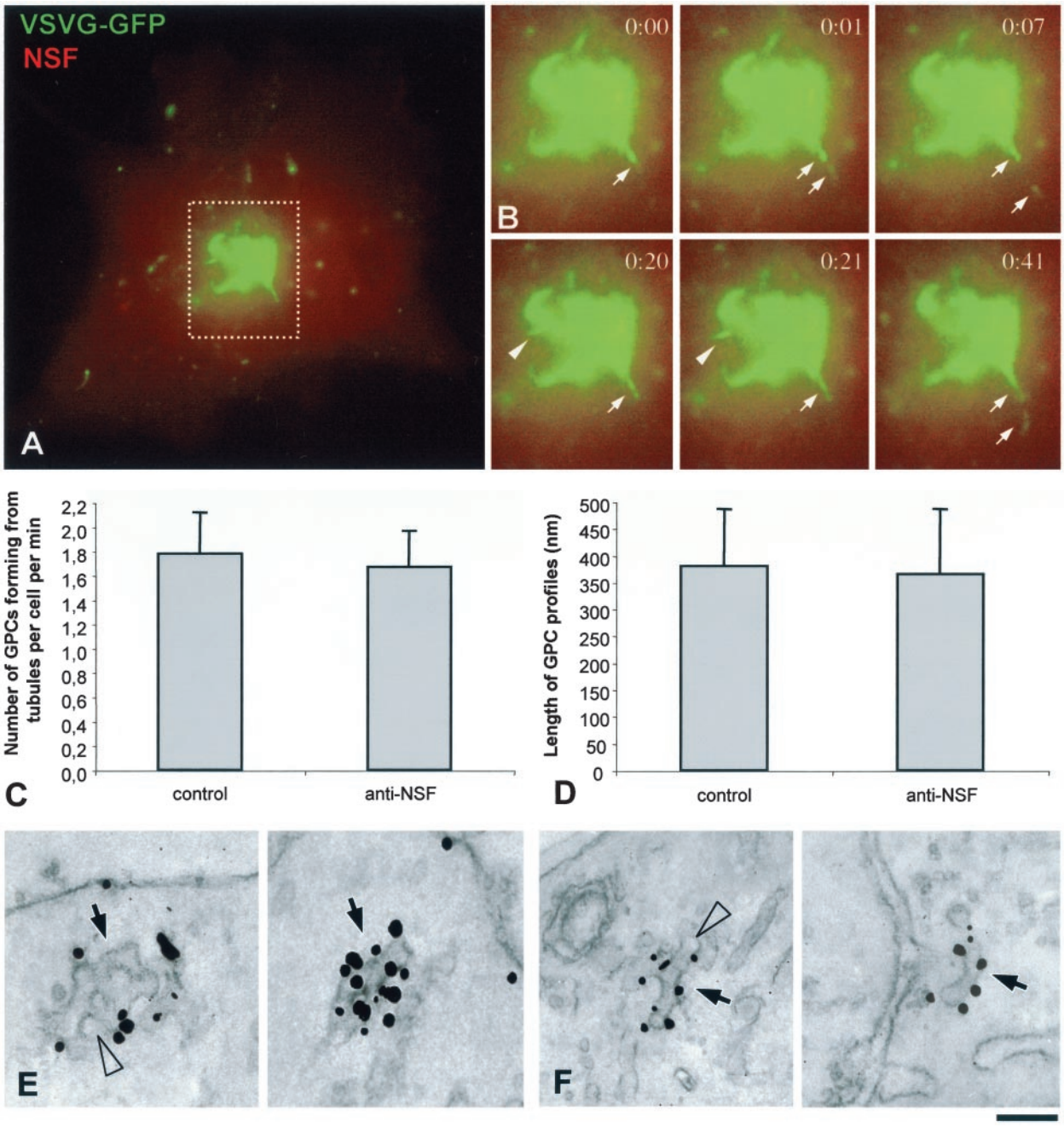

Figure 5. Dynamics and ultrastructure of GPCs in anti-NSF-antibody–microinjected cells. (A) A BHK cell was transfected with VSVG-GFP, exposed to the 40°C block, and microinjected with an anti-NSF antibody (mixed with fluorescent dextran) during the 20°C block. Shortly after the temperature shift to 32°C, the cell was observed in vivo under confocal microscope (Movie 5). (B) Time-lapse images, corresponding to the dashed box region of the cell in A show formation of VSVG-GFP–positive GPCs from tubular precursors (arrows and arrowheads). (C) BHK cells were treated and observed in vivo as in A. The number of GPCs forming from tubular precursors per cell per min (mean ± SD) in mock-injected (n = 13) and anti-NSF-antibody-injected (n = 11) cells is shown. (D) BHK cells were infected with VSV, exposed to the 40°C block, and microinjected during the 20°C block. Thirty minutes after the 20°C block release, they were fixed, labeled for VSVG by using the immunogold protocol, and prepared for EM. GPC profiles were found in thin sections and their length (mean ± SD) was measured in mock-injected (n = 15) and anti-NSF-antibody-injected (n = 15) cells. (E and F). Immuno-gold labeling of VSVG reveals that the morphology of GPCs (arrows) is similar in control (D) and anti-NSF-antibody-injected (E) cells. Arrowheads indicate fenestrae within GPCs. Bar, 7 μm (A), 4.5 μm (B), and 95 nm (E and F).

To demonstrate in a more direct way that PC-I aggregates are incorporated into VSVG-positive GPC precursors, HFs were transfected with VSVG-GFP and 10 min after the 20°C block release they were observed under confocal microscope. Figure 6, E and G, show the formation of typical GPC precursors from the Golgi (see also Movie 6). After fixing and immunolabeling, exactly the same precursors and the GPCs derived from them were seen to contain PC-I (Figure

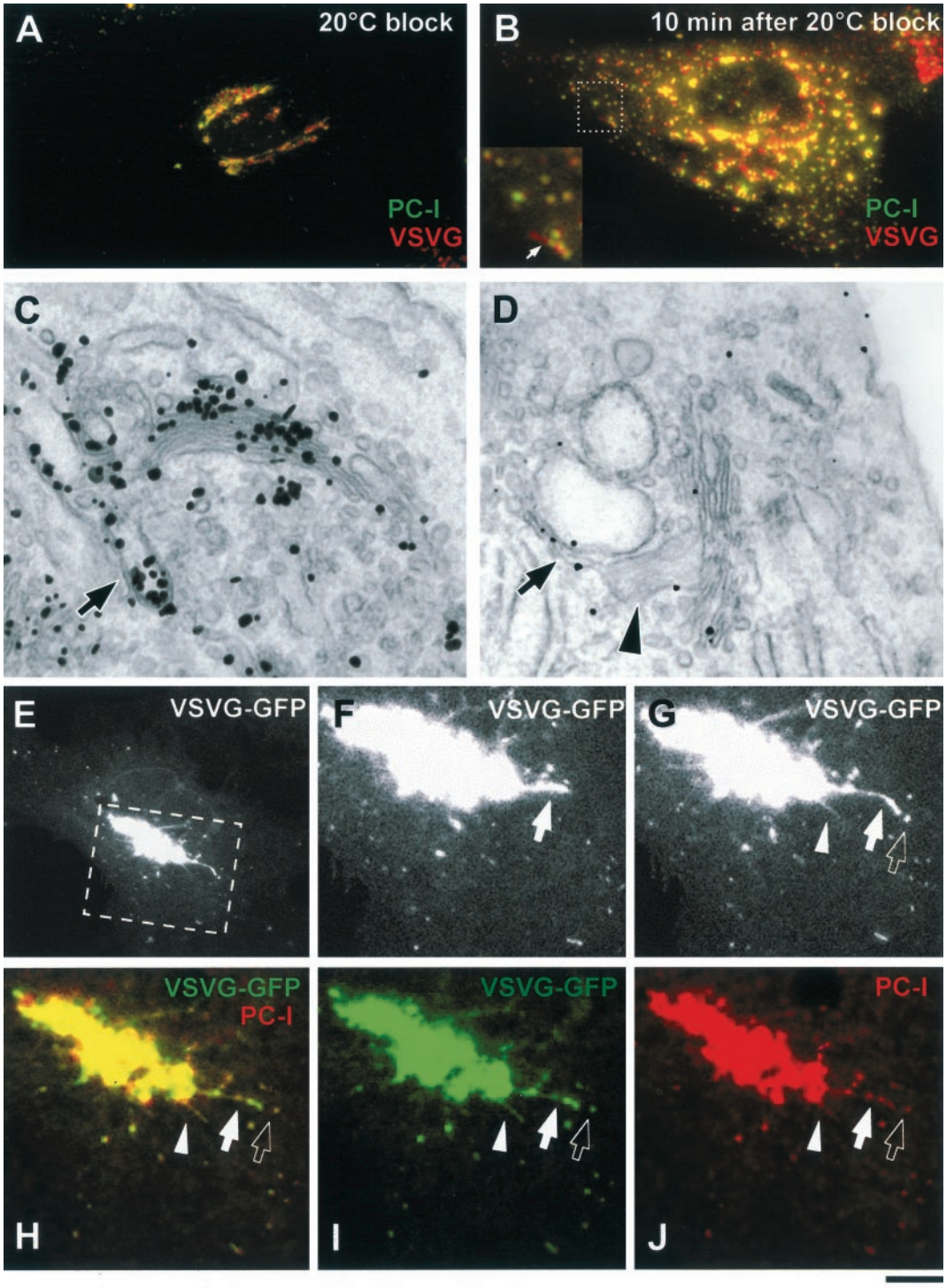

Figure 6. VSVG and PC-I exit the Golgi within the same GPCs. (A) HFs were infected with VSV, exposed to the 40 and 20°C blocks, and stained with antibodies against VSVG and PC-I. Both VSVG and PC-I reside within the Golgi after the 20°C block. (B) HFs as in A, 10 min after the release of the 20°C block, both VSVG and PC-I are found within the same GPCs. Inset, detail with arrows indicating a GPC where VSVG and PC-I exhibit an overlap only within the globular part of the GPC, whereas the tubular part of the GPC contains VSVG alone. (C) HFs, infected and treated as in A, were fixed, stained against VSVG by using the immunogold protocol, and prepared for EM. Gold particles reveal the accumulation of VSVG within the Golgi stack and together with PC-I in extensions (arrow). (D) HFs as in C, after the release of the 20°C block; PC-I extensions (arrowhead) and VSVG are found in common large tubular-saccular carriers (arrow, arrowhead) peeling off the Golgi stack. (E) Formation of a GPC was observed in the Golgi region (dashed box) of a HF transfected with VSVG-GFP and exposed subsequently to the 40 and 20°C blocks (Movie 6). (F and G) Time-lapse images, corresponding to the dashed box region of the cell in E, show a tubular GPC precursor (arrow, arrowhead) extending from the Golgi and a GPC (empty arrow) derived from one of them. (H–J) The same GPC precursor in C was fixed and stained for PC-I. Immunolabeling indicates the presence of PC-I within both GPC precursors (arrow, arrowhead) and free GPCs (empty arrow) that had pinched off one of the precursors. Bar, 7.2 μm (A and B), 200 nm (C), 270 nm (D), 8 μm (E), and 3.9 μm (F–J).

6, H–J), indicating that both proteins leave the Golgi within the same structures.

Direct Visualization of GPC Precursor Ultrastructure during Protrusion from the Golgi

Although the above-mentioned results suggested no role of fusion in the process of GPC assembly, we wanted to analyze the ultrastructure of GPC precursors because this might provide additional insight in understanding how GPCs form. For example, to draw conclusions about the mechanisms of GPC formation, it is important to understand whether GPC precursors are simple linear tubules, as they seem at the light microscopy level, or whether they comprise complex tubular-reticular TGN-like membranes. In fact, a simple tubule can be pulled from the flat surface of a cisterna by a mechanical force, whereas formation of TGN-like membranes requires the membrane bending machinery (see DISCUSSION).

To analyze the ultrastructure of GPC precursors, the previously described CVEM approach was used (Mironov *et al*., 2000; Polishchuk *et al*., 2000; Polishchuk and Mironov, 2001). A VSVG-GFP tubule was monitored under the confocal microscope while it extended for 2.5 μm from the edge of the Golgi near the border of the nucleus (Figure 7A; Movie 7). As noted above, all tubules protruding beyond this length end up forming bona fide GPCs; this tubule is therefore representative of a GPC precursor. The cell was fixed before detachment of a GPC from this tubular precursor and then processed for immuno-EM (see MATERIALS AND METHODS). Serial sections demonstrated that the precursor was composed of mostly tubular membranes, lying close to the nucleus (Figure 7, B–E, arrows) and connected to the Golgi complex (Figure 7, B–D, white asterisks). However, these tubules were not simple linear structures. Instead, this GPC precursor comprised complex branching and fenestrated membranes (Figure 7E, inset), with morphological features strikingly reminiscent of those of the TGN itself (compare, for example, inset in Figure 7E with box in Figure 9A). Another GPC tubular precursor (Figure 8A, arrow; Movie 8) was fixed when it had extended for 3 μm toward the nucleus, and was then found in thin sections (Figure 8, B and C, arrows). Immunoperoxidase-EM showed that the initial part of this GPC precursor looked like a fenestrated tubular-saccular membrane segment, continuous with the parent membranes of the Golgi stack (Figure 8C, inset arrows). The tip of this GPC precursor comprised complex interconnected tubular membranes (Figure 8C, arrows) corresponding to the fluorescent hot spot in the confocal image (Figure 8A, arrow). VSVG-GFP-containing vesicles were not detected among the membranes composing either of the above-mentioned two GPC precursors.

Together, 19 GPC precursors that exhibited variable morphologies and sizes were analyzed by CVEM, with all revealing tubular-reticular features. These ultrastructural features strongly suggest that they were pieces of the TGN still attached to the Golgi stack and that they were pulled and unfolded into the neighboring cytoplasm while still remaining connected to the Golgi cisterna. Therefore, these features agree well with the concept that GPCs are formed by scission of large domains of TGN membranes.

A further tool to capture multiple GPC formation sites is the use of a PKD mutant that blocks detachment of GPC precursors from Golgi membranes (Liljedahl *et al*., 2001). Cells transfected with this PKD mutant were then analyzed by EM and seen to exhibit large VSVG- and TGN46-positive tubules, which were unable to detach from the central Golgi

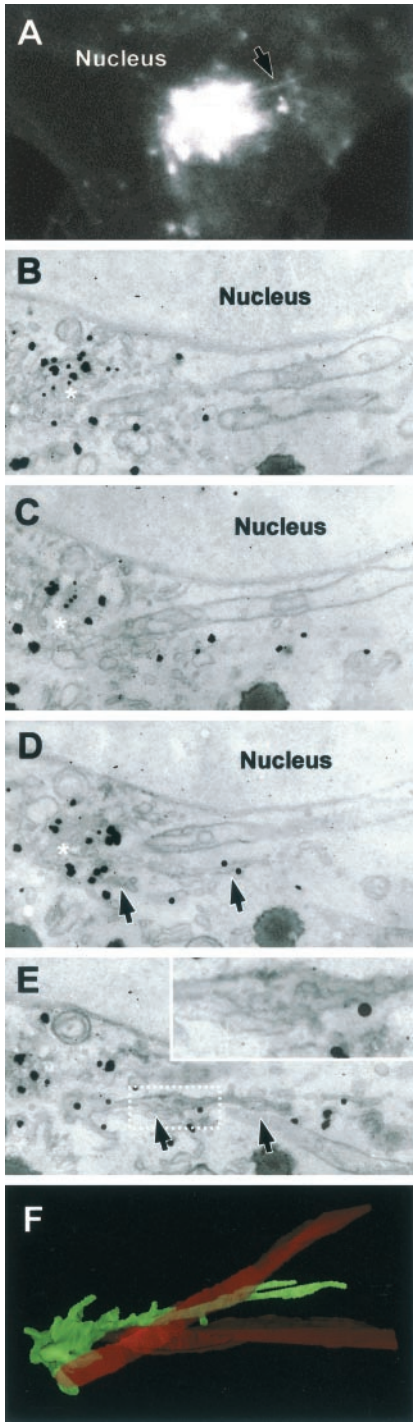

Figure 7. CVEM of a GPC formation site. (A) A VSVG-GFP-transfected Cos7 cell was observed in vivo after the release of the 20°C block and fixed when a GPC precursor (arrow) was seen to extend from the Golgi, along the border of the nucleus (Movie 7). (B–E) After anti-VSVG immunogold labeling, the same cell was embedded in resin and cut into serial sections. The membranes of the same GPC precursor (arrow in D and E) were found in serial sections (B–E). Arrows indicate the membranes of the GPC precursor and its connection with the parent Golgi membranes (white asterisk). Inset in E, detail of the dashed box region in E, showing a complex portion of the GPC precursor containing fenestrae. (F) Three-dimensional reconstruction of the same GPC precursor (green) and a surrounding mitochondrion (red) from the serial sections. Bar, 4.2 μm (A), 560 nm (B–E), 530 nm (F).

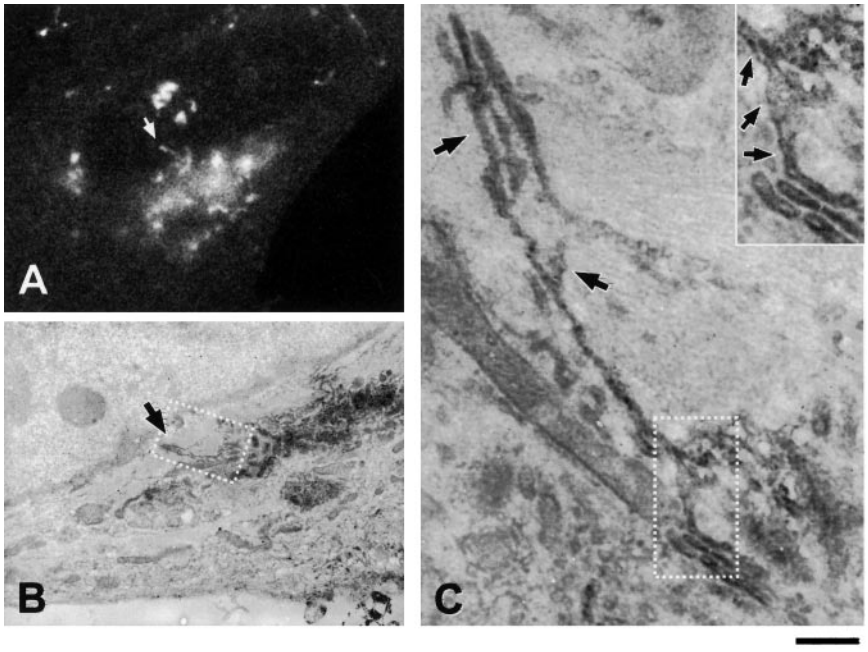

Figure 8. Ultrastructure of a GPC formation site. (A) Thirty minutes after the release of the 40°C block, a VSVG-GFP–transfected HF was fixed at the moment when a GPC precursor extended from the Golgi (arrow; Movie 8). (B) The same cell was labeled with an antibody against VSVG using the immuno-peroxidase protocol, and processed for CVEM. The same GPC formation site (arrow) was found at low EM magnification. (C) Corresponding to the dashed box region of the cell in B, the arrows indicate complex segments of the GPC precursor. Inset, detail of the area defined by the dashed box region in C. Arrows in inset show continuity between the GPC precursor and parent Golgi membranes. Bar, 7.5 μm (A), 3 μm (B), 375 nm (C), and 230 nm (inset).

body (our unpublished data). By EM, these structures looked similar to the GPC formation sites captured by CVEM.

VSVG Does Not Undergo Coat-mediated Concentration upon Exit from the TGN

The exit of proteins, such as MPR and furin, from the TGN is associated with their concentration in clathrin-coated buds (Klumperman *et al*., 1993; Dittie *et al*., 1999). However, qualitative observations (e.g., Figure 7) did not indicate higher levels of VSVG in tubular precursors than in TGN membranes. Moreover, the GPC precursors described here are structurally very different from clathrin buds, suggesting a different mechanism of formation. We therefore wanted to establish quantitatively whether VSVG exits the TGN by bulk flow or via a coat-mediated concentration-coupled step. The approaches were 1) to compare the density of VSVG in the TG-TGN with that in GPCs after their detachment from the TGN; and 2) to test whether adaptor or coat proteins are recruited to the GPC precursors.

To quantify the density of cargo at the EM level, VSVG-infected Cos7 cells were kept at 20°C for the accumulation of VSVG in the Golgi (Figure 9, A and C) and then fixed either immediately or 10 min after the release of the block (Figure 9, B and D). After fixing, VSVG was labeled using the nanogold or cryo-immunogold protocols. At 20°C, VSVG was present throughout the TGN (Figure 9, A and C), with the exception of clathrin-coated buds (Figure 9C, arrowhead), and in many of the cisternae of the Golgi stack (Figure 9, A and C). On release of the temperature block, VSVG occurred within complex tubular-saccular-reticular GPCs in peripheral parts of the cell (Figure 9, B and D, arrows). A comparison of the densities of gold particles did not demonstrate statistically significant differences between GPCs and the TGN (Table 1). To rule out potential artifacts due to the temperature block, similar measurements were also performed in VSV-infected cells kept for 4 h at 32°C. Also in these cells, which contained ~2.5-fold less VSVG, the density of gold particles did not indicate an increase in VSVG concentration during passage from the TGN into GPCs (Table 1).

To examine whether known coat proteins associate with GPC precursors, VSVG-GFP tubular extensions growing out of the Golgi were fixed and stained with antibodies against γ-, δ-, and ϵ-adaptins, components of the adaptor protein (AP)1, AP3, and AP4 complexes, respectively. All three markers labeled peripheral cytosolic structures, and to some extent the Golgi, but did not label GPC precursors or free GPCs (Figure 9E). Similar to APs, clathrin, β-COP, and GGA adaptors (Movie 9) were not detected at the forming GPCs.

These results indicate that GPC formation is not coupled to cargo concentration by known coat proteins and support a bulk flow mode of VSVG export from the TGN. This behavior clearly differs from that of MPR, which exhibited a marked concentration within small, apparently coated, zones, as visualized by cryo-immuno-EM (Figure 9C, arrowhead; see also Klumperman *et al*., 1993).

Table 1. Density of VSVG within *trans*-Golgi/TGN and GPCs

	trans-Golgi/TGN	GPCs
Nanogold		
20°C block release	17.4 ± 4.7	18.4 ± 5.2
Steady state[a]	7.6 ± 3.1	8.6 ± 3.8
Cryogold		
20°C block release	11.2 ± 4.3	11.0 ± 3.6
Steady state[a]	3.8 ± 2.2	4.4 ± 2.8

Linear density of gold labeling for VSVG expressed as the number of gold particles per micrometer of membrane length. Values represent means ± SDs obtained by analyzing 25 cells (nanogold) and 18 cells (cryogold).

[a] Cells were infected with VSV, kept for 4 h at 32°C, and then fixed for EM.

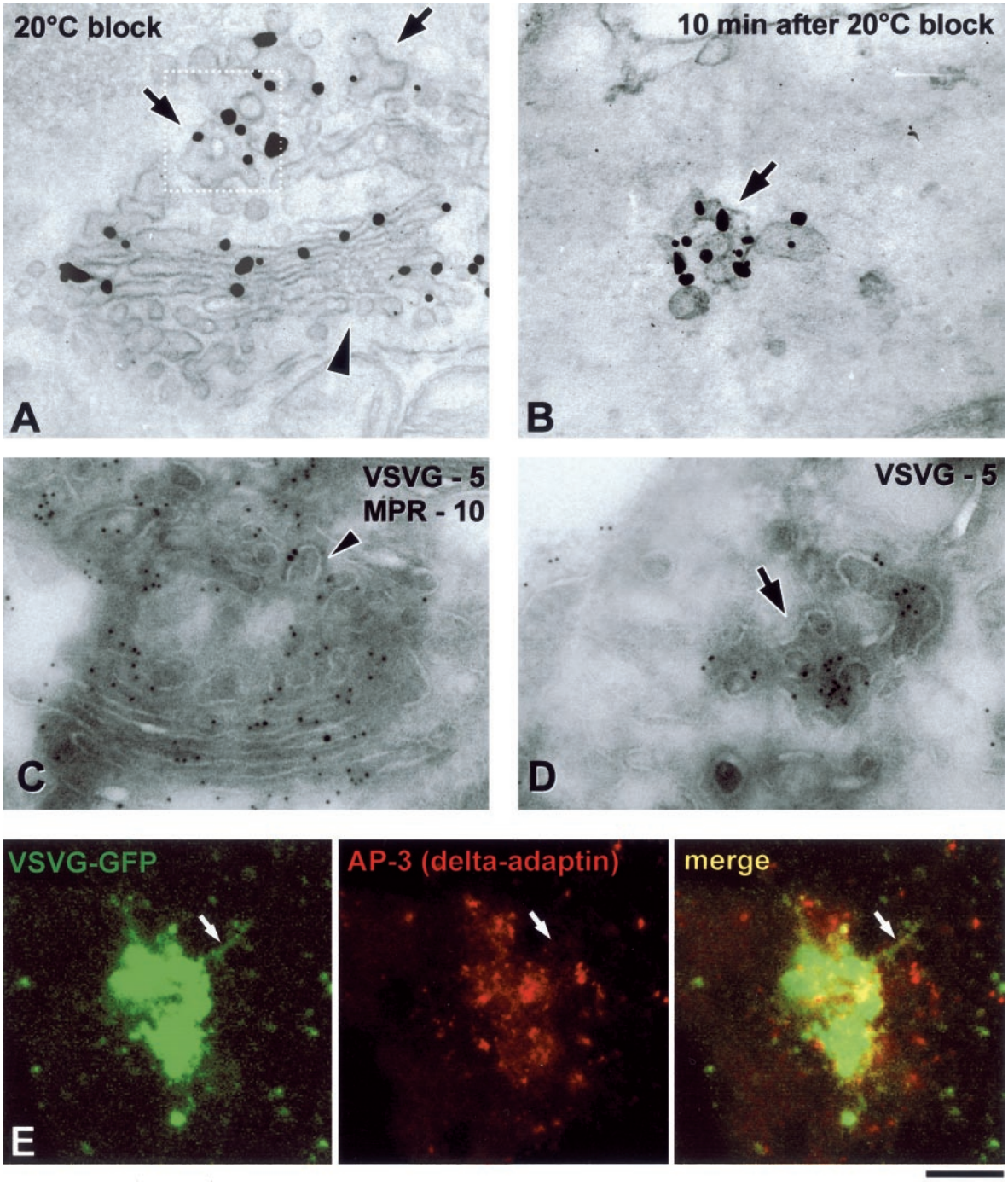

Figure 9. Distribution of VSVG and adaptor proteins upon exit from the Golgi. (A and B) VSV-infected Cos7 cells were fixed at the end of the 20°C block (A) or shortly after the shift to 32°C (B) and stained with an anti-VSVG antibody for immuno-EM. A similar density of gold particles is seen on the TGN (A, arrows) and the free GPC (B, arrow), with a lesser extent of labeling at the *cis*-face of the Golgi stack (A, arrowhead). (C and D) VSV-infected Cos7 cells were fixed at the end of the 20°C block (C) or 10 min after the block release (D) and prepared for cryo-immuno-EM with anti-VSVG and anti-MPR antibodies. VSVG (5-nm gold) is distributed throughout the TGN membranes (C), except at coated profiles where MPR (10-nm gold) resides (arrowhead). A GPC (D, arrow) exhibits a similar density of VSVG labeling as the TGN (C). (E) A VSVG-GFP–transfected Cos7 cell was exposed to the 40 and 20°C blocks. The cell was shifted to 32°C, fixed at the moment when a GPC precursor started to extend from the Golgi, and stained with an antibody against α-tubulin. Immunostaining revealed that the GPC precursor (arrow) does not contain δ-adaptin. Bar, 200 nm (A–D) and 4 μm (E).

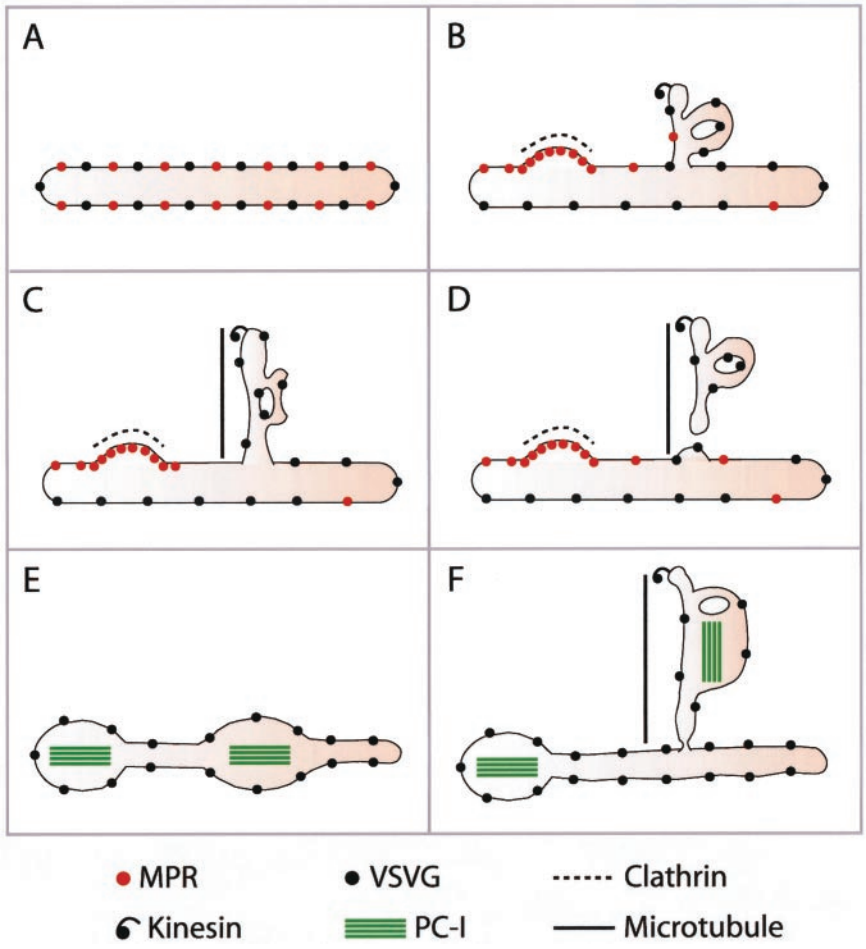

Figure 10. Model of GPC formation and related cargo sorting at the TGN. (A) TGN membrane with VSVG and MPR before GPC formation. (B) Part of the TGN membrane bends, tubulates, and acquires the MT docking device (kinesin, thus becoming a GPC precursor. MPR is segregated from the bulk TGN into clathrin-coated domains. (C) The GPC precursor docks onto a MT and is extruded out of the Golgi. (D) The GPC precursor undergoes fission, and the resulting GPC moves away. (E) The TGN membrane with VSVG and PC-I aggregates before formation of the GPC precursor. (F) On formation of the GPC precursor, both VSVG and PC-I aggregates are incorporated into its membranes.

DISCUSSION

This study addresses the mechanisms of formation of constitutive GPCs by using a cluster of morphological approaches developed for the study of the morpho-functional organization of traffic in intact cells. GPCs are large tubular pleiomorphic containers that can sometimes be several micrometers in length, or as large as half a Golgi cisterna (Polishchuk *et al.*, 2000). Here, we report that these carriers emerge from the Golgi through a bulk flow process involving the formation of tubular TGN cargo domains that later detach en block from the TGN after being pulled out of the Golgi along MTs (see model in Figure 10).

The above-mentioned conclusions rest on three main lines of evidence: 1) direct observations by CVEM showing that GPC precursors are morphologically very similar to the TGN and remain connected with the parent TGN membranes while they are extruded from the Golgi, with small vesicles being scarce or absent at these formation sites; 2) the demonstration that treatments blocking membrane (and thus vesicle) fusion do not affect the formation of GPCs; and 3) the observations that the same GPCs contain both the diffusible traffic marker VSVG, and PC-I aggregates that are too large to enter vesicles. Collectively, these results provide compelling evidence in support of the model proposed above.

These conclusions might apply to other (Lippincott-Schwartz *et al.*, 2000), but not necessarily all, cargo proteins. For example, the formation of PM-directed carriers containing the Semliki Forest virus glycoproteins is sensitive to NSF-mediated fusion inhibitors (Band *et al.*, 2001). However, Semliki Forest virus glycoproteins pass though the endocytic compartment before exiting for the PM (Sariola *et al.*, 1995). No such traffic step has been reported in the case of VSVG. Thus, the findings of Band *et al.* (2001) and ourselves are not in direct conflict; rather, together they support the concept that there are different routes from the TGN to the PM (Sariola *et al.*, 1995). On the other hand, other cargoes, such as GPI-GFP (Nichols *et al.*, 2001), the p75 neutrophin receptor (Kreitzer *et al.*, 2000) and TGN46 (this study) also seem to leave the Golgi in tubule-like carriers of variable sizes. Most of these proteins, however, have so far been studied only at the light microscopy level.

Mechanism of Formation and Cleavage of GPC Precursors at the TGN

Because GPC formation does not involve the budding and then fusion of small vesicles, there remain two main possibilities regarding their generation. The first is that they might form essentially by the mechanical pulling force of MT-based motors exerted on a flat, parent membrane surface (e.g., a TGN or TG saccule or cisterna). This has been shown to be mechanistically possible for both artificial and natural membranes (Roux *et al.*, 2002). If this is the case, GPCs would be expected to be essentially simple linear

tubular structures (Roux *et al*., 2002). The second possibility is that these precursors are tubular subdomains of the TGN, generated before docking and extrusion by MTs. In this case, GPCs should reflect the morphologically complex structure of their parent membranes. Our observations provide support in favor of the latter scheme. Indeed, both free GPCs and GPC precursors comprise complex tubular-reticular-saccular structures very similar to the main components of the TGN in many cell types (Clermont *et al*., 1995). GPCs even exhibit bona fide fenestrae; again, a typical feature of the Golgi and the TGN (Rambourg and Clermont, 1990).

These observations raise the question of the mechanisms by which the highly bent tubular-reticular GPC precursors are generated, because it seems unlikely that these structures could be induced exclusively by the coat proteins involved in the formation of traditional round vesicles. The potential candidates are numerous, and include lipid-metabolizing enzymes such as phospholipase A_2 (Brown *et al*., 2003), transmembrane lipid transporters (flippases) (Sprong *et al*., 2001), proteins able to bend membranes into flexible tubules, possibly similar to amphiphysin or endophilin (Farsad *et al*., 2001), and others (Sprong *et al*., 2001). Much work will be needed to establish which, if any, of these molecules are responsible for the formation of GPC precursors.

After formation, GPCs must detach from the Golgi to travel to the PM. The fission mechanisms at the TGN are still unclear, and several potential protein candidates are being investigated, including PKD, dynamin, phospholipid transfer proteins, phospholipase D, CtBP3/BARS, and phosphatidylinositol kinases (reviewed in Corda *et al*., 2002). Our data suggest another candidate mechanism for tubule fission, i.e., tubule stretching, because they indicate that at least a facilitating role in fission might be played by a mechanical, MT-mediated pulling force. A few observations are significant in this respect. One is that when tubular GPC precursors stop moving during their elongation (i.e., when they are not being stretched), sometimes for many seconds, they never undergo cleavage at that time. Cleavage occurs only when movement resumes, i.e., when the tubules are being stretched. That a degree of tension is likely to exist in the GPC tubular precursors is indicated by the observations (this study and Hirschberg *et al*., 1998) that when a GPC detaches, the remaining portion still connected to the Golgi usually retracts elastically toward the Golgi mass. Another observation suggesting a role for tubule tension in fission is that tubule cleavage usually occurs between complex domains of the GPC precursor (hot spots in fluorescence recordings; Figure 1); tension within these segments can be generated locally as individual hot spots of the same GPC precursor contain kinesin and can slide along the MT at different speeds (see RESULTS). Thus, segments of a GPC precursor between two such kinesin-containing zones can undergo stretching and become preferential sites for fission.

Mechanistically, there is more than one way in which tension could facilitate fission. Certain proteins are known to be able to insert better into lipid films when tension is applied (reviewed in Burger, 2000). Thus, distended membranes could provide preferred "docking" sites for molecules such as CtBP/BARS (our unpublished data), PKD (Liljedahl *et al*., 2001), and/or dynamin (Cao *et al*., 2000; Kreitzer *et al*., 2000), all of which have been proposed to be involved in the process of GPC fission from the Golgi. In addition, it is possible that tension might deform membranes in ways that could directly promote the fission process.

Export of VSVG-containing Cargo Domains from the TGN Is a Bulk Flow Process

GPC precursors do not measurably concentrate VSVG and remain in physical continuity with the TGN membranes. At the same time, GPCs exclude other TGN proteins, such as MPR, syntaxin 6, and furin, indicating that a segregation process has taken place. How can there be segregation without the concentration of VSVG? We propose the following hypothesis: some specialized cargoes, such as MPR and furin, segregate into relatively small TGN domains in which they undergo coat-mediated concentration before exit. For instance, the AP1 adaptor can drive a strong concentration of MPR (Doray *et al*., 2002; this study) and >50% of the total Golgi MPR is associated with AP-1–positive clathrin-coated membranes (Klumperman *et al*., 1993; this study). Similarly, other cargoes, such as furin (Dittie *et al*., 1999) and Lamp-1 (Honing *et al*., 1996), concentrate in relatively small clathrin-coated domains. VSVG, however, resides throughout the entire TGN structure, with the exception of clathrin-coated buds (Griffiths *et al*., 1985; present study). Thus, the exclusion of VSVG from such buds might not result in a detectable increase in VSVG concentration in GPC precursors (see scheme of GPC formation in Figure 10, A–D) because the volume of these buds is too small to measurably reduce the volume accessible to VSVG itself. To our knowledge, this would be the first documented case of exit by bulk flow from the TGN.

Given the above-mentioned information, what is the role for coat proteins in the export of VSVG? On the one hand, our data indicate that clathrin, AP1, AP3, AP4, and GGAs are excluded from GPC precursors. This is in line with previous reports showing the absence of coat and APs on already formed carriers (Hirschberg *et al*., 1998; Polishchuk *et al*., 2000). Moreover, blockade of the AP1, AP3, and clathrin budding machineries has been reported not to affect the secretion of constitutive cargo proteins, although it alters the trafficking of lysosomal proteins (Dell' Angelica *et al*., 1999; Rehling *et al*., 1999; Hirst *et al*., 2000). On the other hand, it has recently been shown that VSVG interacts with the δ-subunit of the AP3 complex and that this facilitates (but it is not necessary for) VSVG transport from the Golgi to the PM (Nishimura *et al*., 2002). We cannot exclude that although undetectable under our conditions, a low capacity AP3-dependent export mechanism might exist. However, our data clearly indicate that majority of VSVG is certainly transported by bulk flow. Another potential candidate coat protein for VSVG export in polarized cells is the AP1B complex, which plays an important role in correct targeting of cargo proteins from the Golgi to the basolateral portion of the PM (Folsch *et al*., 2001). However, AP1B is expressed only in polarized epithelia (Ohno *et al*., 1999), and we have used nonpolarized cells throughout the present study.

Conclusions and Perspectives

From the present analysis, a working model of GPC formation can be proposed in which three main stages can be distinguished (see model in Figure 10). The first (and most complex) step is the formation of a mature tubular-reticular cargo domain in the TGN. This step is not coupled to VSVG concentration and involves the local bending of TGN membranes into tubular-reticular networks. This also requires the exclusion of resident proteins and of molecules destined to the endosomes (by concentration into separate small coated domains), and the inclusion of the appropriate machinery in the membrane destined for export. The second stage is the

kinesin-mediated docking and extension of these tubular domains along MTs. The third and final step is the en block fission of this domain from the rest of the TGN, which could be facilitated by traction-induced tension.

These conclusions have a bearing not only on our view of the morpho-functional organization of cargo export from the TGN but also on our understanding of the molecular mechanisms underlying exit from the Golgi. The challenge is now to design in vitro assays that can reconstitute various stages of the TGN export process and to thus help to elucidate the identity and function of the underlying molecular machineries.

ACKNOWLEDGMENTS

We thank all those who provided us with antibodies and cDNAs; O. Martella and P. Nicoziani for assistance with PC-I experiments; G. Di Tullio for the preparation of the α-SNAP protein; A.A. Mironov, M.A. DeMatteis, M.M. Kozlov, and K.N.J. Burger for helpful discussions; C.P. Berrie for critically reading of the manuscript; and R. Le Donne, E. Fontana, and A. Cavallo for excellent secretarial assistance and artwork preparation. We acknowledge financial support from the Associazione Italiana Ricerca sul Cancro (Milan, Italy) and Telethon Italy (grants E.0982 and E.1249). E.V.P. is supported by an Alfredo Leonardi Fellowship for rare disease (Mario Negri Institute for Pharmacological Research, Milan, Italy).

REFERENCES

Acharya, U., Jacobs, R., Peters, J.M., Watson, N., Farquhar, M.G., and Malhotra, V. (1995). The formation of Golgi stacks from vesiculated Golgi membranes requires two distinct fusion events. Cell *82*, 895–904.

Band, A.M., Maatta, J., Kaariainen, L., and Kuismanen, E. (2001). Inhibition of the membrane fusion machinery prevents exit from the TGN and proteolytic processing by furin. FEBS Lett. *505*, 118–124.

Bannykh, S.I., and Balch, W.E. (1997). Membrane dynamics at the endoplasmic reticulum–Golgi interface. J. Cell Biol. *138*, 1–4.

Banting, G., and Ponnambalam, S. (1997). TGN38 and its orthologues: roles in post-TGN vesicle formation and maintenance of TGN morphology. Biochim. Biophys. Acta *1355*, 209–217.

Brown, W.J., Chambers, K., and Doody, A. (2003). Phospholipase A2 (PLA2) enzymes in membrane trafficking: mediators of membrane shape and function. Traffic *4*, 214–221.

Burger, K.N. (2000). Greasing membrane fusion and fission machineries. Traffic *1*, 605–613.

Cao, H., Thompson, H.M., Krueger, E.W., and McNiven., M.A. (2000). Disruption of Golgi structure and function in mammalian cells expressing a mutant dynamin. J. Cell Sci. *113*, 1993–2002.

Clermont, Y., Rambourg, A., and Hermo, L. (1995). Trans-Golgi network (TGN) of different cell types: three-dimensional structural characteristics and variability. Anat. Rec. *242*, 289–301.

Corda, D., Hidalgo Carcedo, C., Bonazzi, M., Luini, A., and Spanò, S. (2002). Molecular aspects of membrane fission in the secretory pathway. Cell. Mol. Life Sci. *59*, 1819–1832.

Dell'Angelica, E.C., Shotelersuk, V., Aguilar, R.C., Gahl, W.A., and Bonifacino, J.S. (1999). Altered trafficking of lysosomal proteins in Hermansky-Pudlak syndrome due to mutations in the beta 3A subunit of the AP-3 adaptor. Mol. Cell *3*, 11–21.

Dittie, A.S., Klumperman, J., and Tooze, S.A. (1999). Differential distribution of mannose-6-phosphate receptors and furin in immature secretory granules. J. Cell Sci. *112*, 3955–3966.

Doray, B., Ghosh, P., Griffith, J., Geuze, H.J., and Kornfeld, S. (2002). Cooperation of GGAs and AP-1 in packaging MPRs at the trans-Golgi network. Science *297*, 1700–1703.

Farsad, K., Ringstad, N., Takei, K., Floyd, S.R., Rose, K., and De Camilli, P. (2001). Generation of high curvature membranes mediated by direct endophilin bilayer interactions. J. Cell Biol. *155*, 193–200.

Fisher, L.W., Stubbs, J.T. 3rd, and Young, M.F. (1995). Antisera and cDNA probes to human and certain animal model bone matrix noncollagenous proteins. Acta Orthop. Scand. Suppl. *266*, 61–65.

Folsch, H., Pypaert, M., Schu, P., and Mellman, I. (2001). Distribution and function of AP-1 clathrin adaptor complexes in polarized epithelial cells. J. Cell Biol. *152*, 595–606.

Fukunaga, T., Furuno, A., Hatsuzawa, K., Tani, K., Yamamoto, A., and Tagaya, M. (1998). NSF is required for the brefeldin A-promoted disassembly of the Golgi apparatus. FEBS Lett. *435*, 237–240.

Griffiths, G., and Hoppeler, H. (1986). Quantitation in immunocytochemistry: correlation of immunogold labeling to absolute number of membrane antigens. J. Histochem. Cytochem. *34*, 1389–1398.

Griffiths, G., Pfeiffer, S., Simons, K., and Matlin, K. (1985). Exit of newly synthesized membrane proteins from the trans cisterna of the Golgi complex to the plasma membrane. J. Cell Biol. *101*, 949–964.

Griffiths, G., and Simons, K. (1986). The trans Golgi network: sorting at the exit site of the Golgi complex. Science *234*, 438–443.

Hirschberg, K., Miller, C.M., Ellenberg, J., Presley, J.F., Siggia, E.D., Phair, R.D., and Lippincott-Schwartz, J. (1998). Kinetic analysis of secretory protein traffic and characterization of Golgi to plasma membrane transport intermediates in living cells. J. Cell Biol. *143*, 1485–1503.

Hirst, J., Lui, W.W., Bright, N.A., Totty, N., Seaman, M.N., and Robinson, M.S. (2000). A family of proteins with gamma-adaptin and VHS domains that facilitate trafficking between the trans-Golgi network and the vacuole/lysosome. J. Cell Biol. *149*, 67–80.

Honing, S., Griffith, J., Geuze, H.J., and Hunziker, W. (1996). The tyrosine-based lysosomal targeting signal in lamp-1 mediates sorting into Golgi-derived clathrin-coated vesicles. EMBO J. *15*, 5230–5239.

Keller, P., and Simons, K. (1997). Post-Golgi biosynthetic trafficking. J. Cell Sci. *110*, 3001–3009.

Keller, P., Toomre, D., Diaz, E., White, J., and Simons, K. (2001). Multicolour imaging of post-Golgi sorting and trafficking in live cells. Nat. Cell Biol. *3*, 140–149.

Klumperman, J., Hille, A., Veenendaal, T., Oorschot, V., Stoorvogel, W., von Figura, K., and Geuze, H.J. (1993). Differences in the endosomal distributions of the two mannose 6-phosphate receptors. J. Cell Biol. *121*, 997–1010.

Kreitzer, G., Marmorstein, A., Okamoto, P., Vallee, R., and Rodriguez-Boulan, E. (2000). Kinesin and dynamin are required for post-Golgi transport of a plasma-membrane protein. Nat. Cell Biol. *2*, 125–127.

Ladinsky, M.S., Wu, C.C., McIntosh, S., McIntosh, J.R., and Howell, K.E. (2002). Structure of the Golgi and distribution of reporter molecules at 20 degrees C reveals the complexity of the exit compartments. Mol. Biol. Cell *13*, 2810–2825.

Liljedahl, M., Maeda, Y., Colanzi, A., Ayala, I., Van Lint, J., and Malhotra, V. (2001). Protein kinase D regulates the fission of cell surface destined transport carriers from the trans-Golgi network. Cell *10*, 409–420.

Lippincott-Schwartz, J., Roberts, T.H., and Hirschberg, K. (2000). Secretory protein trafficking and organelle dynamics in living cells. Annu. Rev. Cell Dev. Biol. *16*, 557–589.

Mironov, A.A., *et al*. (2001). Small cargo proteins and large aggregates can traverse the Golgi by a common mechanism without leaving the lumen of cisternae. J. Cell Biol. *155*, 1225–1238.

Mironov, A.A., Polishchuk, R.S., and Luini, A. (2000). Visualizing membrane traffic in vivo by combined video fluorescence and 3-D electron microscopy. Trends Cell Biol. *10*, 349–353.

Mostov, K.E., Verges, M., and Altschuler, Y. (2000). Membrane traffic in polarized epithelial cells. Curr. Opin. Cell Biol. *12*, 483–490.

Nichols, B.J., Kenworthy, A.K., Polishchuk, R.S., Lodge, R., Roberts, T.H., Hirschberg, K., Phair, R.D., and Lippincott-Schwartz, J. (2001). Rapid cycling of lipid raft markers between the cell surface and Golgi complex. J. Cell Biol. *153*, 529–541.

Nishimura, N., Plutner, H., Hahn, K., and Balch, W.E. (2002). The delta subunit of AP-3 is required for efficient transport of VSV-G from the trans-Golgi network to the cell surface. Proc. Natl. Acad. Sci. USA *99*, 6755–6760.

Ohno, H., Tomemori, T., Nakatsu, F., Okazaki, Y., Aguilar, R.C., Foelsch, H., Mellman, I., Saito, T., Shirasawa, T., and Bonifacino, J.S. (1999). Mu1B, a novel adaptor medium chain expressed in polarized epithelial cells. FEBS Lett. *449*, 215–220.

Polishchuk, R.S., and Mironov, A.A. (2001). Correlative video/light electron microscopy. In: Current Protocols in Cell Biology, ed. J.S. Bonifacino, M. Dasso, J.B. Harford, J. Lippincott-Schwartz, and K.M. Yamada, John Wiley & Sons, New York, 4.8.1–4.8.9.

Polishchuk, R.S., Polishchuk, E.V., Marra, P., Buccione, R., Alberti, S., Luini, A., and Mironov, A.A. (2000). GFP-based correlative light-electron micros-

copy reveals the saccular-tubular ultrastructure of carriers in transit from the Golgi apparatus to the plasma membrane. J. Cell Biol. *148*, 45–58.

Rabouille, C., Kondo, H., Newman, R., Hui, N., Freemont, P., and Warren, G. (1998). Syntaxin 5 is a common component of the NSF- and p97-mediated reassembly pathways of Golgi cisternae from mitotic Golgi fragments in vitro. Cell *92*, 603–610.

Rambourg, A., and Clermont, Y. (1990). Three-dimensional electron microscopy: structure of the Golgi apparatus. Eur. J. Cell Biol. *51*, 189–200.

Rehling, P., Darsow, T., Katzmann, D.J., and Emr, S.D. (1999). Formation of AP-3 transport intermediates requires Vps41 function. Nat. Cell Biol. *1*, 346–353.

Rothman, J.E., and Wieland, F.T. (1996). Protein sorting by transport vesicles. Science *272*, 227–234.

Roux, A., Cappello, G., Cartaud, J., Prost, J., Goud, B., and Bassereau, P. (2002). A minimal system allowing tubulation with molecular motors pulling on giant liposomes. Proc. Natl. Acad. Sci. USA *99*, 5394–5399.

Sariola, M., Saraste, J., and Kuismanen, E. (1995). Communication of post-Golgi elements with early endocytic pathway: regulation of endoproteolytic cleavage of Semliki Forest virus p62 precursor. J. Cell Sci. *108*, 2465–2475.

Sprong, H., van der Sluijs, P., and van Meer, G. (2001). How proteins move lipids and lipids move proteins. Nat. Rev. Mol. Cell. Biol. *2*, 504–513.

Toomre, D., Keller, P., White, J., Olivo, J.C., and Simons, K. (1999). Dual-color visualization of trans-Golgi network to plasma membrane traffic along microtubules in living cells. J. Cell Sci. *112*, 21–33.

White, J., Keller, P., and Stelzer, E.H. (2001). Spatial partitioning of secretory cargo from Golgi resident proteins in live cells. BMC Cell Biol. *2*, 19.